H^∞ control of the neutral point in 3-phase 4-wire DC-AC converters*

Qing-Chang Zhong† and George Weiss
Dept. of Electrical & Electronic Engineering
Imperial College of Science, Technology, and Medicine
Exhibition Rd., London, SW7 2BT, UK

Abstract

We propose a circuit topology and the corresponding H^∞ control design for generating the neutral point in a 3-phase 4-wire DC-AC power converter, which can be connected to loads and/or to the power grid. The neutral point is balanced with respect to the two DC source terminals (as required, for example, in three-level converters). Our design offers significant advantages: the neutral point and the three-phase converter can be controlled independently and there is no need for large capacitors. The controller is designed using H^∞ techniques, which leads to very small deviations of the neutral point from the mid-point of the DC source, in spite of the possibly large neutral current.

Index Terms: DC-AC power converter, multi-level PWM converter, DC-link balancing, neutral line, 3-phase 4-wire power system, H^∞ control

1 Introduction

DC to three-phase AC converters are used in many applications, such as uninterruptible power supplies or small power generating units (possibly using renewable energy sources). In these converters, there is often a need to generate a neutral line, on which the voltage is balanced with respect to the two terminals of the DC power source. Providing such a neutral line is called *DC-link balancing.* If two equal DC sources are present, connected in series, then of course this problem does not arise. However, often only one DC source is present, for example, if the DC voltage is obtained by rectifying a variable frequency AC voltage, produced by a generator.

The neutral line is usually needed on the AC side of the converter to provide a current path for the zero-sequence current components, which could be large if the load is unbalanced or nonlinear. For grid-connected DC to AC converters, the zero-sequence current components could be the result of an unbalanced grid. Another situation where a balanced neutral point is required is in multi-level pulse width modulation (PWM) converters, which have the potential to improve the total harmonic distortion and to reduce the voltage stress across the switches, see [1, 2, 3, 4] and the survey paper [5].

If the neutral line is not well controlled and the neutral current has strong low-frequency components, then the neutral current causes the neutral point to deviate severely from the mid-point of the DC source. This deviation of the neutral point may result in an unbalanced or modulated output voltage, the presence of zero-sequence voltage components, and hence an even larger neutral current. Thus, the generation of a balanced neutral point efficiently and simply has now become an important problem. Although DC to 3-phase 3-wire electronic power converters have been widely studied in recent years, see [6, 7], DC to 3-phase 4-wire converters have been discussed in only a few papers, such as [8, 9].

A straightforward way to provide the neutral point is to use two capacitors, in parallel with large balancing resistors, as shown in Figure 1(a). Such a configuration is called a *split DC link.* Since the neutral current flows through the capacitors, very high capacitance is needed to make the voltage ripple on the capacitors small. Another drawback is that the neutral point usually drifts and becomes non-balanced (when the neutral current has a DC component). Hence, this topology is not suitable for DC-AC converters which supply power to possibly unbalanced consumers or to the grid. Since the neutral current in active power filters does not have a DC component and the fundamental component is relatively small, the split DC link is widely used in active power filters, see for example [10, 11]. Some special PWM generating schemes have been developed for three-level converters to balance the charging

*This research was supported by the EPSRC (Grant No. GR/N38190/1).
†Corresponding author, *Tel*: 0044-20-7594 6295, *Fax*: 0044-20-7594 6282, *e-mail*: zhongqc@ic.ac.uk, *URL*: http://members.fortunecity.com/zhongqc.

of the balancing capacitors, see [3, 12, 13] (these converters do not provide a neutral line on the AC side, hence there is no neutral current). In this case, if the load current contains some harmonics, the balance cannot be maintained no matter how large the capacitors are, as discussed in [12].

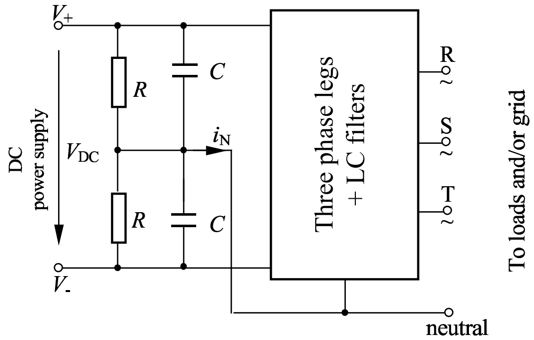

(a) The split DC link

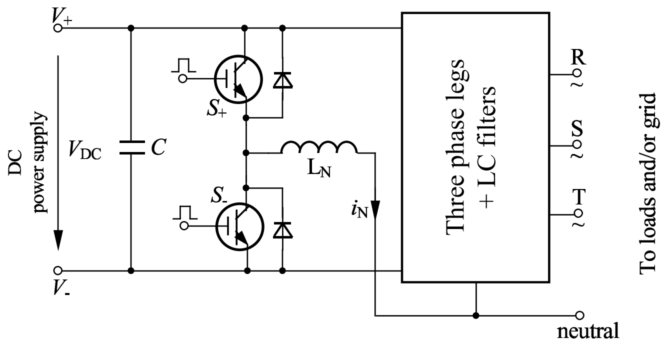

(b) The neutral leg as used with three-dimensional space vector modulation

Figure 1: Conventional topologies to generate the neutral line

A better way to provide the neutral point is to add an additional fourth leg, called a *neutral leg*, to the conventional three-leg converter [8], as shown in Figure 1(b). An interesting control strategy for this circuit, called *three-dimensional space vector modulation*, was presented in [9]. In this strategy, the requirement of having the neutral line balanced with respect to the two terminals of the DC power supply is entirely dropped: we end up with high voltages at high frequencies on the two DC terminals (with respect to the neutral line), so that the DC terminals may become an EMI source. An advantage of this control strategy, as compared to the split DC link, is that the output AC voltage can be about 15% higher (for a given DC link voltage). However, the additional neutral leg cannot be independently controlled to maintain the neutral point and hence the corresponding control design (including the PWM waveform generating scheme) becomes much more complicated, as pointed out in [9].

This paper proposes a circuit topology and a simple and efficient controller for DC-link balancing. The circuit, as shown in Figure 2, combines the two circuits shown in Figure 1. The significant improvement in this topology is that the phase legs and the neutral leg can be controlled independently. In this circuit, the majority of the neutral current no longer flows through the DC link capacitors and thus high capacitances are not needed, saving volume and cost. Simulations show that the neutral point can be balanced even when the load of the three-phase converter is extremely unbalanced. Moreover, our controller can cope with the variations of the DC-link voltage.

A similar circuit has been proposed very recently in [14], by combining a DC-DC buck converter and a DC-DC boost converter. The buck converter is used to increase the neutral point voltage; the boost converter is used to lower it. A comparator (possibly with hysteresis) is used to activate one or the other of these two DC-DC converters. In this case, the controller is nonlinear and there will be a steady-state error. The possibility of a large neutral current is not discussed in [14] (actually, we think that the control strategy of [14] is not suitable for a large neutral current).

2 The neutral leg circuit and its modeling

The circuit in Figure 2 consists of a DC to 3-phase AC converter (typically containing three phase legs), a neutral leg, an inductor and two capacitors. The controller generates the firing pulses to open or to close the switches S_+ and S_-, in a complementary way. The general aim of the controller is to maintain the mid-point of the DC source V_{ave} very close to the neutral point. If the DC-link voltage is constant, then the controller achieves this by maintaining the inductor current i_L equal to the neutral current i_N so that no current flows through the capacitors. Thus, the capacitors maintain constant and equal voltages and hence, the neutral point remains balanced. However, the controller can also cope with a variable DC-link voltage, as we shall see. From the control point of view, the two capacitors C_{N1} and C_{N2} need not be equal, in particular, one of them could be zero. However, usually a filtering of the DC source is desirable, which can be achieved by putting both capacitors.

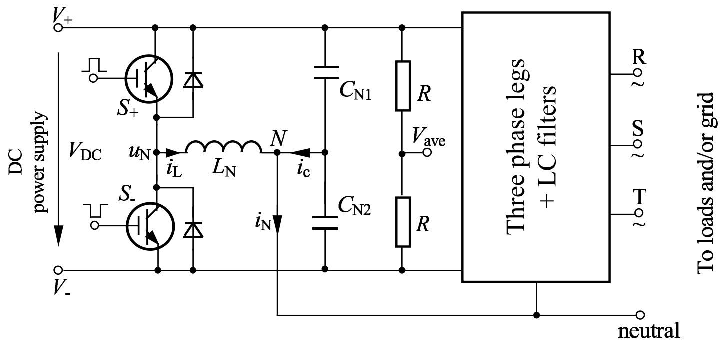

Figure 2: The proposed neutral leg circuit

All voltages are measured with respect to the neutral point N. The *DC-link voltage* is

$$V_{DC} = V_+ - V_-, \tag{1}$$

and the mid-point (or average) of the DC source, which is desired to be 0, is

$$V_{ave} = \frac{V_+ + V_-}{2}. \tag{2}$$

Using Kirchhoff's laws, we obtain the following equations:

$$u_N = L_N \frac{di_L}{dt} + R_N i_L, \qquad i_N = i_L + i_c \tag{3}$$

where R_N is the equivalent series resistance of the inductor, and

$$i_c = C_{N1} \frac{dV_+}{dt} + C_{N2} \frac{dV_-}{dt}. \tag{4}$$

Actually, equations (1) and (2) determine a coordinate transformation

$$\begin{bmatrix} V_+ \\ V_- \end{bmatrix} = \begin{bmatrix} 0.5 & 1 \\ -0.5 & 1 \end{bmatrix} \begin{bmatrix} V_{DC} \\ V_{ave} \end{bmatrix}.$$

Hence, (4) can be re-formulated as

$$i_c = (C_{N1} + C_{N2}) \frac{dV_{ave}}{dt} + \frac{C_{N1} - C_{N2}}{2} \frac{dV_{DC}}{dt}.$$

Define a new voltage variable (actually, a disturbance)

$$V_0 = -\frac{C_{N1} - C_{N2}}{C_{N1} + C_{N2}} \frac{V_{DC}}{2}, \tag{5}$$

which reflects the effect of the possibly unequal capacitors C_{N1} and C_{N2} and the effect of the possible variations of V_{DC}. Then the last formula for i_c becomes

$$i_c = (C_{N1} + C_{N2}) \frac{d(V_{ave} - V_0)}{dt}. \tag{6}$$

Denote the *switching frequency* by f_s, so that $h = 1/f_s$ is the *switching period*. We introduce the following signal:

$$q = \begin{cases} 1 & \text{if } S_+ \text{ is on and } S_- \text{ is off,} \\ -1 & \text{if } S_- \text{ is on and } S_+ \text{ is off.} \end{cases}$$

The shape of this signal and of the corresponding u_N is shown in Figure 3. We denote the average of q over a switching period by p, so that $p \in [-1, 1]$. Then the *duty cycle* of S_+ is

$$d = \frac{1+p}{2}$$

and the average of u_N over a switching period (assuming that V_+ and V_- are constant within a switching period) is

$$average(u_N) = dV_+ + (1-d)V_- = \frac{p}{2}V_{DC} + V_{ave}.$$

Employing the averaging technique common in power electronics, we obtain the approximate equation

$$u_N = \frac{p}{2}V_{DC} + V_{ave}. \tag{7}$$

Combining (3), (6) and (7), the block diagram of the neutral leg system is shown in Figure 4. V_0 plays the role of an external disturbance, while p is the control variable. Strictly speaking, even this simplified model is nonlinear, because p is multiplied with the variable V_{DC}. However, since the variations of V_{DC} are relatively small, in the design we will consider that V_{DC} appearing in the first block in Figure 4 is equal to its nominal value V_{DC}^{nom}. If the variations of V_{DC} are expected to be large, then they can be compensated by measuring V_{DC} and multiplying the output p of the controller with the correction factor V_{DC}^{nom}/V_{DC} (however, simulations show that the effect of this correction is not significant).

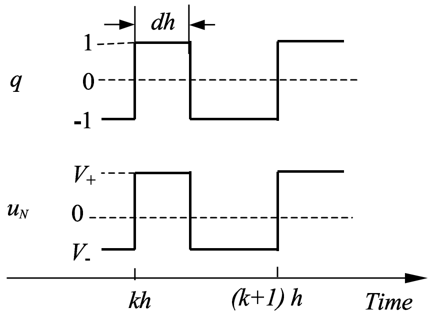

Figure 3: The signals q (top line) and u_N (bottom line)

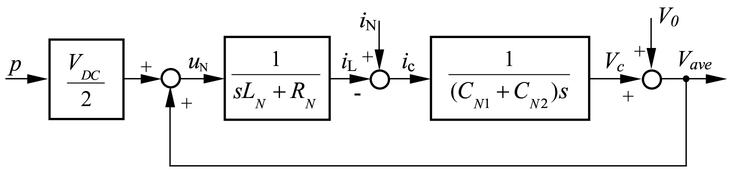

Figure 4: Block diagram of the uncontrolled neutral leg system

3 Controller design

The control objective for the plant in Figure 4 is to maintain a stable and balanced neutral point, i.e., to make V_{ave} as small as possible while maintaining the stability of the system. The disturbances are the neutral current i_N and the equivalent external disturbance V_0 defined in (5). Since the current i_c contains much ripple (at the switching frequency), it must be sensed through a low-pass filter F, as shown in Figure 5. The remaining ripple after this filter will be interpreted as a measurement noise n, see again Figure 5. We denote the Laplace transformation by a hat. Then V_i, the signal available to the controller from the measurement of i_c, is given by $\hat{V}_i = F\hat{i}_c + \hat{n}$. From the H^∞ control point of view, the simplest formulation of the problem would be to minimize the H^∞-norm of the transfer function from $\begin{bmatrix} i_N & V_0 & n \end{bmatrix}^T$ to the average voltage V_{ave}. Such a formulation would be unrealistic, since it would ignore the fact that the disturbances are expected in a certain frequency range and it would not reflect that we must avoid the signal u_N getting too large (because for obvious physical reasons, $V_- < u_N < V_+$). Thus, as is usual in applications of the H^∞ theory, we introduce the weighting functions W_v to multiply V_{ave} and W_u to multiply u_N. We also introduce two new variables I_0 and I_n, which are proportional to V_0 and n via the factors ρ and ζ. These weighting factors are needed to adjust the relative importance of the three disturbances i_N, V_0 and n in the H^∞-norm minimization process (because i_N, I_0 and I_n will have equal importance). The H^∞ control problem is then formulated to minimize the H^∞-norm of the transfer function from $w = \left[\begin{array}{ccc} i_N & I_0 & I_n \end{array}\right]^T$ to $z = \left[\begin{array}{cc} V_v & V_u \end{array}\right]^T$, denoted $\mathbf{T}_{zw} = \mathcal{F}_l(\mathbf{P}, \mathbf{K})$. The closed-loop system can be represented in terms of Laplace transforms, ignoring initial conditions, as

$$\left[\begin{array}{c} \hat{z} \\ \hat{y} \end{array}\right] = \mathbf{P} \left[\begin{array}{c} \hat{w} \\ \hat{u} \end{array}\right], \qquad \hat{u} = \mathbf{K}\,\hat{y},$$

where $\mathbf{P}$ is the generalized plant and $\mathbf{K}$ is the controller to be designed. A nearly optimal $\mathbf{K}$ can be obtained by the H^∞ control algorithm (which solves two Riccati equations at each iteration), see [15, 16] for details. In the sequel we derive the realization of $\mathbf{P}$ (which is needed to obtain $\mathbf{K}$) and the realization of the closed-loop transfer function from $\left[\begin{array}{ccc} i_N & V_0 & n \end{array}\right]^T$ to $\left[\begin{array}{cc} V_{ave} & u_N \end{array}\right]^T$.

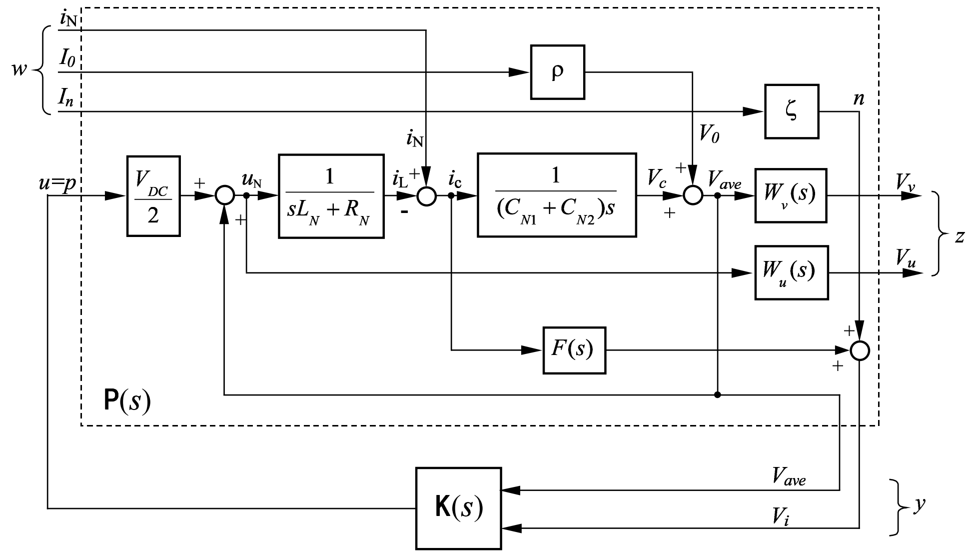

Figure 5: The H^∞ control problem is to minimize the norm of the transfer function from w to z. The weighting functions W_v and W_u need not be implemented physically, they are only mathematical tools.

3.1 The realization of P

If the state variables of the original plant are chosen to be the inductor current i_L and the voltage $V_c = V_{ave} - V_0$, i.e., $x = \left[\begin{array}{c} i_L \\ V_c \end{array}\right]$, and if the control input u is p, then the following state equations can be obtained from Figure 5:

$$\dot{x} = Ax + B_1 w + B_2 u \tag{8}$$

where

$$A = \left[\begin{array}{cc} -\frac{R_N}{L_N} & \frac{1}{L_N} \\ -\frac{1}{C_{N1}+C_{N2}} & 0 \end{array}\right], \quad B_1 = \left[\begin{array}{ccc} 0 & \frac{\rho}{L_N} & 0 \\ \frac{1}{C_{N1}+C_{N2}} & 0 & 0 \end{array}\right], \quad B_2 = \left[\begin{array}{c} \frac{V_{DC}}{2L_N} \\ 0 \end{array}\right].$$

The output equations are

$$\begin{aligned} V_{ave} &= C_a x + D_{1a} w + D_{2a} u, \\ u_N &= C_{1b} x + D_{11b} w + D_{12b} u, \\ i_c &= C_{2b} x + D_{21b} w + D_{22b} u, \end{aligned} \tag{9}$$

where

$$C_a = \left[\begin{array}{cc} 0 & 1 \end{array}\right], \quad D_{1a} = \left[\begin{array}{ccc} 0 & \rho & 0 \end{array}\right], \quad D_{2a} = \left[\begin{array}{c} 0 \end{array}\right],$$

$$C_{1b} = \left[\begin{array}{cc} 0 & 1 \end{array}\right], \quad D_{11b} = \left[\begin{array}{ccc} 0 & \rho & 0 \end{array}\right], \quad D_{12b} = \left[\begin{array}{c} \frac{V_{DC}}{2} \end{array}\right],$$

$$C_{2b} = \begin{bmatrix} -1 & 0 \end{bmatrix}, \quad D_{21b} = \begin{bmatrix} 1 & 0 & 0 \end{bmatrix}, \quad D_{22b} = \begin{bmatrix} 0 \end{bmatrix}.$$

Assume that the realization of the weighting function W_v is

$$W_v = \left[\begin{array}{c|c} A_v & B_v \\ \hline C_v & D_v \end{array}\right]$$

(this notation means that $W_v(s) = D_v + C_v(sI - A_v)^{-1}B_v$, see for example [15]). Then

$$\begin{aligned}
\hat{V}_v &= \left[\begin{array}{c|c} A_v & B_v \\ \hline C_v & D_v \end{array}\right] \hat{V}_{ave} \\
&= \left[\begin{array}{c|c} A_v & B_v \\ \hline C_v & D_v \end{array}\right] \left[\begin{array}{c|cc} A & B_1 & B_2 \\ \hline C_a & D_{1a} & D_{2a} \end{array}\right] \begin{bmatrix} \hat{w} \\ \hat{u} \end{bmatrix} \\
&= \left[\begin{array}{cc|cc} A & 0 & B_1 & B_2 \\ B_v C_a & A_v & B_v D_{1a} & B_v D_{2a} \\ \hline D_v C_a & C_v & D_v D_{1a} & D_v D_{2a} \end{array}\right] \begin{bmatrix} \hat{w} \\ \hat{u} \end{bmatrix}
\end{aligned} \tag{10}$$

(recall that a hat is used to denote the Laplace transformation). Similarly, assume that the realization of the weighting function W_u is

$$W_u = \left[\begin{array}{c|c} A_u & B_u \\ \hline C_u & D_u \end{array}\right],$$

then

$$\begin{aligned}
\hat{V}_u &= \left[\begin{array}{c|c} A_u & B_u \\ \hline C_u & D_u \end{array}\right] \hat{u}_N \\
&= \left[\begin{array}{cc|cc} A & 0 & B_1 & B_2 \\ B_u C_{1b} & A_u & B_u D_{11b} & B_u D_{12b} \\ \hline D_u C_{1b} & C_u & D_u D_{11b} & D_u D_{12b} \end{array}\right] \begin{bmatrix} \hat{w} \\ \hat{u} \end{bmatrix}.
\end{aligned} \tag{11}$$

Assume that the implementation of the low-pass filter F is

$$F = \left[\begin{array}{c|c} A_F & B_F \\ \hline C_F & D_F \end{array}\right],$$

then

$$\begin{aligned}
\hat{V}_i &= \left[\begin{array}{c|c} A_F & B_F \\ \hline C_F & D_F \end{array}\right] \hat{i}_c + \zeta \hat{I}_n \\
&= \left[\begin{array}{c|c} A_F & B_F \\ \hline C_F & D_F \end{array}\right] \left[\begin{array}{c|cc} A & B_1 & B_2 \\ \hline C_{2b} & D_{21b} & D_{22b} \end{array}\right] \begin{bmatrix} \hat{w} \\ \hat{u} \end{bmatrix} + \zeta \hat{I}_n \\
&= \left[\begin{array}{cc|cc} A & 0 & B_1 & B_2 \\ B_F C_{2b} & A_F & B_F D_{21b} & B_F D_{22b} \\ \hline D_F C_{2b} & C_F & D_F D_{21b} + \begin{bmatrix} 0 & 0 & \zeta \end{bmatrix} & D_F D_{22b} \end{array}\right] \begin{bmatrix} \hat{w} \\ \hat{u} \end{bmatrix}.
\end{aligned} \tag{12}$$

Combining (8), (9), (10), (11) and (12), we obtain the realization of the generalized plant $\mathbf{P}$, with inputs w, u and outputs z, y, as follows:

$$\mathbf{P} = \left[\begin{array}{cccc|c:c}
A & 0 & 0 & 0 & B_1 & B_2 \\
B_v C_a & A_v & 0 & 0 & B_v D_{1a} & B_v D_{2a} \\
B_u C_{1b} & 0 & A_u & 0 & B_u D_{11b} & B_u D_{12b} \\
B_F C_{2b} & 0 & 0 & A_F & B_F D_{21b} & B_F D_{22b} \\
\hline
D_v C_a & C_v & 0 & 0 & D_v D_{1a} & D_v D_{2a} \\
D_u C_{1b} & 0 & C_u & 0 & D_u D_{11b} & D_u D_{12b} \\
\hdashline
C_a & 0 & 0 & 0 & D_{1a} & D_{2a} \\
D_F C_{2b} & 0 & 0 & C_F & D_F D_{21b} + \begin{bmatrix} 0 & 0 & \zeta \end{bmatrix} & D_F D_{22b}
\end{array}\right].$$

3.2 The realization of the closed-loop transfer function

Denote $z' = \begin{bmatrix} V_{ave} \\ u_N \end{bmatrix}$ and $y = \begin{bmatrix} V_{ave} \\ V_i \end{bmatrix}$ and denote by $\tilde{\mathbf{P}}$ the transfer function from $\begin{bmatrix} w \\ u \end{bmatrix}$ to $\begin{bmatrix} z' \\ y \end{bmatrix}$. Then

$$\tilde{\mathbf{P}} = \left[\begin{array}{cc|c:c} A & 0 & B_1 & B_2 \\ B_F C_{2b} & A_F & B_F D_{21b} & B_F D_{22b} \\ \hline C_a & 0 & D_{1a} & D_{2a} \\ C_{1b} & 0 & D_{11b} & D_{12b} \\ \hdashline C_a & 0 & D_{1a} & D_{2a} \\ D_F C_{2b} & C_F & D_F D_{21b} + \begin{bmatrix} 0 & 0 & \zeta \end{bmatrix} & D_F D_{22b} \end{array}\right] \doteq \left[\begin{array}{c|cc} \tilde{A} & \tilde{B}_1 & \tilde{B}_2 \\ \hline \tilde{C}_1 & \tilde{D}_{11} & \tilde{D}_{12} \\ \tilde{C}_2 & \tilde{D}_{21} & \tilde{D}_{22} \end{array}\right].$$

Assume that the controller to be designed is realized as

$$\mathbf{K} = \left[\begin{array}{c|c} A_K & B_K \\ \hline C_K & D_K \end{array}\right],$$

where, usually, $D_K = 0$ if $\mathbf{K}$ is obtained from the H^∞ algorithm. However, D_K may be non-zero after controller reduction. According to the star-product formula [15], the transfer function from w to z' is

$$\mathbf{T}_{z'w} = \mathcal{F}_l(\tilde{\mathbf{P}}, \mathbf{K}) = \left[\begin{array}{cc|c} \tilde{A} + \tilde{B}_2 \tilde{R} D_K \tilde{C}_2 & \tilde{B}_2 \tilde{R} C_K & \tilde{B}_1 + \tilde{B}_2 \tilde{R} D_K \tilde{D}_{21} \\ B_K R \tilde{C}_2 & A_K + B_K R \tilde{D}_{22} C_K & B_K R \tilde{D}_{21} \\ \hline \tilde{C}_1 + \tilde{D}_{12} D_K R \tilde{C}_2 & \tilde{D}_{12} \tilde{R} C_K & \tilde{D}_{11} + \tilde{D}_{12} D_K R \tilde{D}_{21} \end{array}\right],$$

where

$$\tilde{R} = (I - D_K \tilde{D}_{22})^{-1}, \qquad R = (I - \tilde{D}_{22} D_K)^{-1}.$$

Hence, the closed-loop transfer function from $w' = \begin{bmatrix} i_N \\ V_0 \\ n \end{bmatrix} = \begin{bmatrix} 1 & 0 & 0 \\ 0 & \rho & 0 \\ 0 & 0 & \zeta \end{bmatrix} w$ to z' (this is the relevant closed-loop transfer function in terms of the original variables) is

$$\mathbf{T}_{z'w'} = \mathbf{T}_{z'w} \begin{bmatrix} 1 & 0 & 0 \\ 0 & \frac{1}{\rho} & 0 \\ 0 & 0 & \frac{1}{\zeta} \end{bmatrix}.$$

4 Example

We have worked out the details of the design described above for the neutral leg of a specific DC-AC converter that we are building, to be used in conjunction with a high-frequency AC generator powered by a gas turbine. The ratings of the converter are 3 phase, 230 V, 25 kW. For the other aspects of this work we refer to [17, 18]. In our circuit, the parameters of the neutral leg are: $L_N = 2.5$mH, $R_N = 0.2\Omega$, $C_{N1} = C_{N2} = 4000\mu$F and $V_{DC} = 900$V. The switching frequency is $f_s = 10$kHz.

4.1 Selection of the weighting functions

It is not easy to choose suitable weighting functions for a specific H^∞ control problem. These functions have to reflect the relative weight of different signals, their frequency characteristics, and at the same time they must be chosen such that the problem is solvable. It is difficult to find guidelines on this problem in the literature (some general guidelines are in [15, 16]). The selection of the weighting functions for our H^∞ control problem is detailed below.

The weighting function W_v has to be large for the range of significant disturbance frequencies (50Hz and a few multiples of it) and it has to decay for larger frequencies, since we cannot control those. (Anyway, we do not expect significant high-frequency variations of V_{ave} because the two capacitors will prevent it). The weighting function $W_v(s)$ can be chosen as

$$W_v(s) = g\frac{s + \omega_h}{s + \omega_l} = \left[\begin{array}{c|c} -\omega_l & g \\ \hline \omega_h - \omega_l & g \end{array}\right],$$

where g is a tuning parameter to move the Bode plot of W_v up or down.

The signal u_N is closely related (almost proportional) to $u = p$. We want to prevent u from becoming large, especially at high frequencies. Therefore, the weighting function W_u is chosen small for low frequencies and large for high frequencies. The usual algorithm employed in H^∞ control requires that the matrix $\begin{bmatrix} D_v D_{2a} \\ D_u D_{12b} \end{bmatrix}$ has full column rank. Since $D_{2a} = 0$, D_u cannot be zero. Hence, W_u has to be non-strictly proper. The weighting function W_u can be chosen as

$$W_u(s) = k\frac{s+\omega_l}{s+\omega_h} = \left[\begin{array}{c|c} -\omega_h & k \\ \hline \omega_l - \omega_h & k \end{array}\right],$$

where k is a tuning parameter to move the Bode plot of W_u up or down. In this application, the fundamental frequency is 50Hz and the high frequency components under consideration are up to the 31st harmonic. Therefore, ω_h is chosen to be $10,000$ rad/sec. The Bode plots of the weighting functions $W_u(s)$ and $W_v(s)$ are shown in Figure 6 for $k = 0.01$ and $g = 10$.

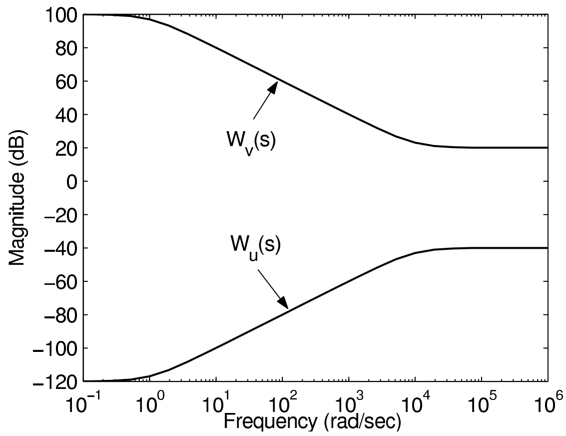

Figure 6: Bode plots of weighting functions

4.2 H^∞ controller design

The tuning parameters are chosen to be: $k = 0.01$, $g = 10$, $\rho = 0.01$ and $\zeta = 0.01$. The weighting parameters are chosen to be $\omega_l = 1$rad/sec and $\omega_h = 10000$rad/sec. Using the μ-analysis toolbox from MATLAB$^{\text{TM}}$, the H^∞ controller $\mathbf{K} = \begin{bmatrix} \mathbf{K}_v & \mathbf{K}_i \end{bmatrix}$ is obtained as

$$\mathbf{K}_v(s) = \frac{-0.0022222(s - 1.383\times10^{11})(s+7.616\times10^4)(s+10^4)(s+120.9)(s+80.08)}{(s+9.799\times10^7)(s+1.117\times10^5)(s+8595)(s+125.2)(s+1)},$$

$$\mathbf{K}_i(s) = \frac{6\times10^8(s+10^4)(s+1000)(s+80)}{(s+9.799\times10^7)(s+1.117\times10^5)(s+8595)(s+125.2)}.$$

This controller is somewhat unrealistic because the sampling frequency is usually limited (in this case, it is chosen the same as the switching frequency, 10kHz). In order to make the controller implementable, any zeros or poles which correspond to a corner frequency much larger than $\omega_h = 10^4$ rad/sec are substituted by a proportional gain (i.e. ignoring s). Then the controller derived earlier is reduced to

$$\mathbf{K}_r(s) = \begin{bmatrix} 2.1384\frac{(s+10^4)(s+120.9)(s+80.08)}{(s+8595)(s+125.2)(s+1)} & 6.123\frac{(s+10^4)(s+1000)(s+80)}{(s+1.117\times10^5)(s+8595)(s+125.2)} \end{bmatrix}.$$

The Bode plots of these controllers are shown in Figure 7. The Bode plots of the corresponding closed-loop transfer functions using the original H^∞ controller $\mathbf{K}$ and the reduced controller $\mathbf{K}_r$ are shown in Figure 8. The curves are so close that they cannot be distinguished.

4.3 Simulation results

The simulation has been carried out in Matlab$^{\text{TM}}$ using the power system blockset. A single-phase leg (buck converter) has been used to create a current i_N flowing back through the neutral line. The reduced controller $\mathbf{K}_r$ has been used in the simulation. The phase leg had a load composed of a resistor $R = 5\Omega$ in series with an inductor $L = 5$mH and it generated a sinusoidal neutral current of about 68A peak at 50 Hz, plus a small ripple at the switching frequency.

Some of the signals have been filtered by a hold filter H, in order to plot them more clearly. Here,

$$H(s) = \frac{1-e^{-sh}}{sh}, \qquad h = 10^{-4}sec. \tag{13}$$

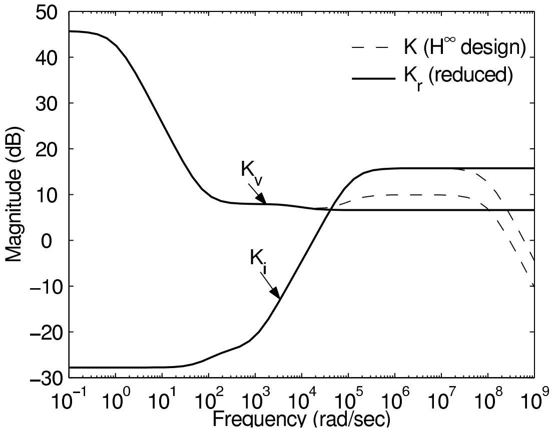

Figure 7: Bode plots of the controllers $\mathbf{K}$ and $\mathbf{K}_r$

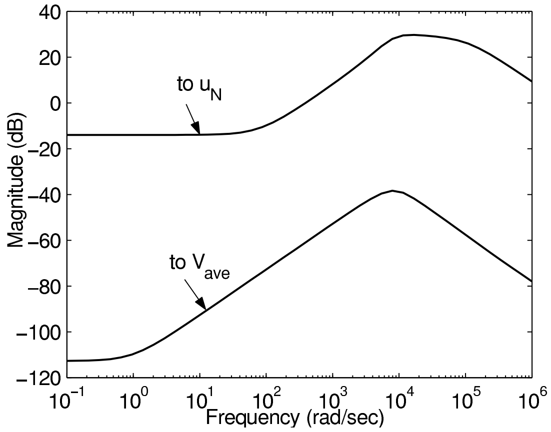

Figure 8: Bode plots of the closed-loop transfer function from i_N to V_{ave} and to u_N

This is a notch filter whose notching frequencies are the switching frequency $f_s = 10$kHz and its nonzero integer multiples. Hence, the effect of the ripple at the switching frequency has been eliminated in some figures. A variable voltage component of $100 \sin 200\pi t$ (Volts) and a resistor of 0.5Ω have been put in series with the DC source of 900 V to make it more realistic. The simulation results are shown in Figure 9. The peak value of V_{ave} is less than 0.1 V; the inductor current is almost the same as the neutral current and the current i_c is very small. The neutral leg provides a voltage u_N of about 60V peak (after hold filtering). The simulations show that the neutral point is balanced with respect to the DC terminals in spite of a varying DC source and a large neutral current.

5 Conclusions

We have presented a new topology for providing a balanced neutral line in 4-wire 3-phase inverters, together with the H^∞ design of the controller. The circuit consists of a conventional neutral leg and a split DC link. The conventional neutral leg provides a path for the neutral current and charges/discharges the capacitors to maintain the neutral point; the capacitors provide a way to independently control the conventional neutral leg and the 3-phase converter. Hence, the role of the split capacitors has been changed from maintaining the neutral point to controlling the neutral point. Actually, only one capacitor is necessary, which results in an asymmetric topology but does not change the control design.

The control of this neutral leg has been formulated as a standard H^∞ control problem. In order to make the H^∞ control problem solvable, an artificial signal (measurement noise) n is introduced. Due to its high bandwidth, the nearly optimal controller has to be reduced so that it can be implemented. The achievable performances are demonstrated in terms of the Bode plots of the closed-loop transfer function as well as simulation results. The simulations show that the neutral point is very accurately balanced with respect to the DC terminals in spite of a varying DC voltage and a large neutral current.

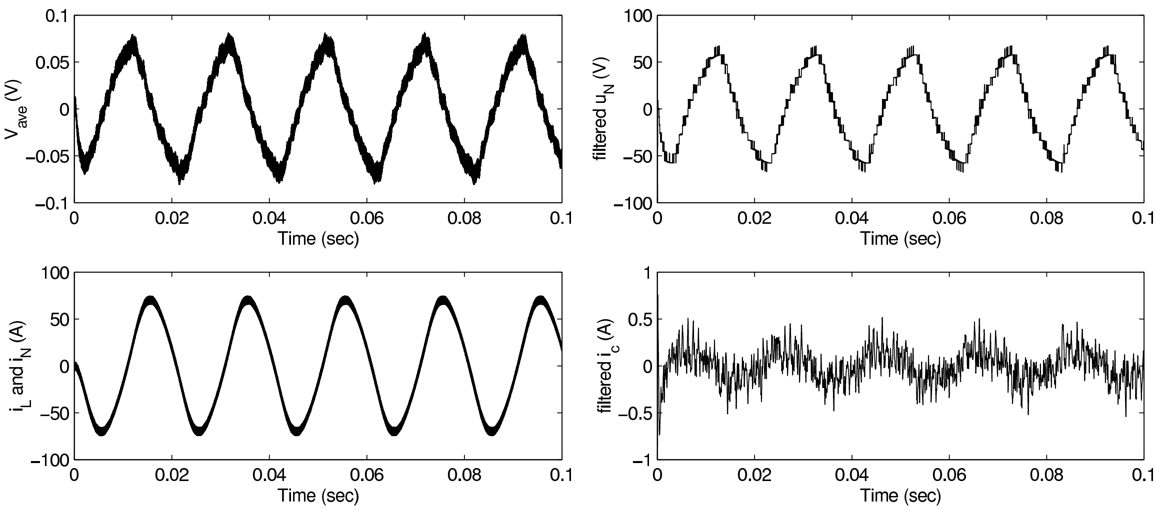

Figure 9: Simulation results. The signals u_N and i_c are only shown after filtering them through the hold filter H from (13), to eliminate the 10 kHz ripple from the plot.

References

[1] D.E. Soto-Sanchez and T.C. Green, "Voltage balance and control in a multi-level unified power flow controller," *IEEE Trans. Power Delivery*, vol. 16, no. 4, pp. 732–738, 2001.

[2] A. Nabae, I. Takahashi, and H. Akagi, "A new neutral-point clamped PWM inverter," *IEEE Trans. Industry Applications*, vol. 17, no. 5, pp. 518–523, 1981.

[3] N. Celanovic and D. Boroyevich, "A comprehensive study of neutral-point voltage balancing problem in three-level neutral-point-clamped voltage source PWM inverters," *IEEE Trans. Power Electronics*, vol. 15, no. 2, pp. 242–249, 2000.

[4] M-C. Wong, Z.-Y. Zhao, Y.-D. Han, and L.-B. Zhao, "Three-dimensional pulse-width modulation technique in three-level power inverters for three-phase four-wired system," *IEEE Trans. Power Electronics*, vol. 16, no. 3, pp. 418–427, 2001.

[5] J. Rodriguez, J.-S. Lai, and F.Z. Peng, "Multilevel inverters: a survey of topologies, controls, and applications," *IEEE Trans. Industrial Electronics*, vol. 49, no. 4, pp. 724–738, 2002.

[6] K.L. Zhou and D. Wang, "Digital repetitive learning controller for three-phase CVCF PWM inverter," *IEEE Trans. Industrial Electronics*, vol. 48, no. 4, pp. 820–830, 2001.

[7] Y. Ito and S. Kawauchi, "Microprocessor-based robust digital control for UPS with three-phase PWM inverter," *IEEE Trans. Power Electronics*, vol. 10, no. 2, pp. 196–204, 1995.

[8] T.M. Jahns, R.W.A.A. De Doncker, A.V. Radun, P.M. Szczesny, and F.G. Turnbull, "System design considerations for a high-power aerospace resonant link converter," *IEEE Trans. Power Electronics*, vol. 8, no. 4, pp. 663–672, 1993.

[9] R. Zhang, D. Boroyevich, V.H. Prasad, H.-C. Mao, F.C. Leeand, and S. Dubovsky, "A three-phase inverter with a neutral leg with space vector modulation," in *Prof. of IEEE Applied Power Electronics Conference and Exposition*, 1997, vol. 2, pp. 857–863.

[10] C.A. Quinn and N. Mohan, "Active filtering of harmonic currents in three-phase, four-wire systems with three-phase and single-phase nonlinear loads," in *Proc. of IEEE Applied Power Electronics Conference and Exposition*, 1992, pp. 829–836.

[11] P. Verdelho and G.D. Marques, "Four-wire current-regulated PWM voltage converter," *IEEE Trans. Industrial Electronics*, vol. 45, no. 5, pp. 761–770, 1998.

[12] D.H. Lee, S.R. Lee, and F.C. Lee, "An analysis of midpoint balance for the neutral-point-clamped three-level VSI," in *Power Electronics Specialists Conference, PESC 98 Record*, 1998, vol. 1, pp. 193 –199.

[13] K.R.M.N. Ratnayake, Y. Murai, and T. Watanabe, "Novel PWM scheme to control neutral point voltage variation in three-level voltage source inverter," in *Conference Record of the IEEE Industry Applications Conference*, 1999, vol. 3, pp. 1950–1955.

[14] A. Von Jouanne, S. Dai, and H. Zhang, "A multilevel inverter approach providing dc-link balancing, ride-through enhancement, and common-mode voltage elimination," *IEEE Trans. Industrial Electronics*, vol. 49, no. 4, pp. 739–745, 2002.

[15] K. Zhou and J.C. Doyle, *Essentials of Robust Control*, Prentice-Hall, Upper Saddle River, N.J., 1997.

[16] M. Green and D.J.N. Limebeer, *Linear Robust Control*, Prentice-Hall, Englewood Cliffs, NJ, 1995.

[17] Q.-C. Zhong, T. Green, J. Liang, and G. Weiss, "Robust repetitive control of grid-connected DC-AC converters," in *Proc. of the 41th IEEE Conf. on Decision & Control*, Las Vegas, Nevada, USA, December 2002.

[18] J. Liang, T. Green, G. Weiss, and Q.-C. Zhong, "Evaluation of repetitive control for power quality improvement of distributed generation," in *Proc. of the 33rd IEEE Annual Power Electronics Specialists Conference*, Queensland, Autralia, June 2002, vol. 4, pp. 1803 –1808.